Solution of the Schrödinger equation for quantum-dot lattices with Coulomb interaction between the dots

M. Taut*
Institute for Solid State and Materials Research Dresden, Postfach 270016, 01171 Dresden, Germany
(Received 10 January 2000)

The Schrödinger equation for quantum-dot lattices with noncubic, non-Bravais lattices built up from elliptical dots is investigated. The Coulomb interaction between the dots is considered in dipole approximation. Then only the center of mass (c.m.) coordinates of different dots couple with each other. This c.m. subsystem can be solved exactly and provides magnetophononlike *collective excitations*. The interdot interaction is involved only through a single interaction parameter. The relative coordinates of individual dots form decoupled subsystems giving rise to *intradot excitation* modes. As an example, the latter are calculated exactly for two-electron dots. Emphasis is layed on *qualitative* effects, like: (i) Influence of the magnetic field on the lattice instability due to interdot interaction; (ii) closing of the gap between the lower and the upper c.m. mode at $B=0$ for elliptical dots due to dot interaction; and (iii) Kinks in the intradot excitation energies (versus magnetic field) due to change of ground-state angular momentum. It is shown that for obtaining striking qualitative effects one should go beyond simple cubic lattices with circular dots. In particular, for observing effects of electron-electron interaction between the dots in far-infrared spectra (breaking Kohn's Theorem) one has to consider dot lattices with at least two dot species with different confinement tensors.

I. INTRODUCTION

Quantum dots have been in the focus of intensive research already for at least a decade which lead to a countless number of publications, therefore we will refer here only to papers which are directly connected to the scope of this work (for a recent book see Ref. 1). Although almost all experiments are performed at dot lattices, in the vast majority of theoretical investigations the interaction between dots is neglected. This is for the following reasons: (i) Because the confinement frequency ω_0 is a parameter, which is mainly extracted from optical properties, it is difficult to tell the influence of dot interaction apart from the intrinsic single dot value. (Possibilities to overcome this problem are discussed in the present work.) (ii) The theory of Raman spectra, which can in principle monitor the dispersion (wave-number dependence) of excitation energies as a direct consequence of interdot interaction, is not yet advanced enough to extract the dispersion. (iii) The lattice constant of dot arrays produced with current technologies is so large (>2000 Å) that large electron numbers N per dot are necessary to obtain a seizable amount of shift. For these N, however, reliable first-principle calculations are not possible. With the advent of self-assembled dot arrays the last item might change.

The scope of this paper is to investigate conditions which lead to *qualitative* and observable effects of interdot interaction on excitation spectra and the phase transition found in Ref. 2. Unlike in Ref. 2, a magnetic field **B** is explicitly taken into account and a microscopic theory is applied. Our approach is purely microscopic, i.e., we solve the Schrödinger equation of a model system *exactly*. Our model comprises the following approximations: (i) The dot confinement is strictly parabolic in radial direction, but with anisotropic confinement frequencies ω_i $(i=1,2)$ and independent of N and **B**. (ii) Overlap of wave functions between different dots is neglected (no hopping). (iii) The Coulomb interaction of the electrons in different dots is treated in dipole approximation (second order in dot diameter over lattice constant). Our model is similar to that in Ref. 3, but allows more complicated dots and lattice structures. Besides, we calculate also the intradot excitations (apart from the collective center-of-mass excitations) for $N=2$ explicitly and discuss the instability[2] in this microscopic model. Our results on the lateral dot dimer are compared with a former paper,[4] which uses a high magnetic field approach, in Sec. III.

The plan of this paper is as follows. For further reference, we briefly summarize in Sec. I some relevant results for one single dot, or for dot lattices, where the distance between the dots is very large. This is important, because all exact solutions in the center-of-mass subsystem are traced back (by special transformations) to the solution of this one-electron Hamiltonian. This is analogous to ordinary molecular and lattice dynamics. After this, we consider a dot dimer, which mimics a lattice, where the dots are pairwise close to each other. This model can give an idea of the effects expected in dot lattices with a basis. Next we consider a rectangular, but primitive lattice in order to obtain the dispersion in the spectra. Finally, the intradot excitations of the Hamiltonian in the relative coordinates are calculated numerically. The paper ends with a summary. In the Appendix we give a short and elementary proof for the fact that the Generalized Kohn Theorem holds even for arbitrary arrays of identical noncircular quantum dots with Coulomb interaction (between the dots) in an homogeneous magnetic field.

II. SINGLE DOT

The Hamiltonian considered here reads (in atomic units $\hbar=m=e=1$)

$$H=\sum_{i=1}^{N}\left\{\frac{1}{2m^*}\left[\mathbf{p}_i+\frac{1}{c}\mathbf{A}(\mathbf{r}_i)\right]^2+\frac{1}{2}\mathbf{r}_i\cdot\mathbf{C}\cdot\mathbf{r}_i\right\}+\frac{1}{2}\sum_{i\neq k}\frac{\beta}{|\mathbf{r}_i-\mathbf{r}_k|},\tag{1}$$

where m^* is the effective mass (in units of the bare electron mass m), β the inverse dielectric constant of the background, and $\mathbf{C}$ a symmetric tensor. In case of a single dot, $\mathbf{C}$ is given by the confinement potential and we define $\mathbf{C}=\mathbf{\Omega}$. It is always possible to find a coordinate system where $\Omega_{12}=\Omega_{21}=0$ and $\Omega_{ii}=\omega_i^2=m^*\omega_i^{*2}$. We use the symmetric gauge $\mathbf{A}=\frac{1}{2}\mathbf{B}\times\mathbf{r}$ throughout.The Zeeman term in H is disregarded at the moment. For $N=1$, the Hamiltonian

$$H=\frac{1}{2m^*}\left[\mathbf{p}+\frac{1}{c}\mathbf{A}(\mathbf{r})\right]^2+\frac{1}{2}\mathbf{r}\cdot\mathbf{C}\cdot\mathbf{r}\tag{2}$$

can be diagonalized exactly. Later on we will see that also the case of interacting dots can be traced back to the solution of type (2). (Therefore we kept the off diagonal elements of $\mathbf{C}$ in the results given below because the dynamical matrix, which also contributes to $\mathbf{C}$, is generally nondiagonal and we want to use the same coordinate system for all $\mathbf{q}$ values.) After transforming the operators $\mathbf{r}_i$ and $\mathbf{p}_i$ to creation-annihilation operators (see, e.g., Ref. 1) and using the procedure described by Tsallis,[6] we obtain for the eigenvalues

$$E(n_+,n_-)=\left(n_++\frac{1}{2}\right)\omega_++\left(n_-+\frac{1}{2}\right)\omega_-;\qquad n_\pm=0,1,2,\ldots,\tag{3}$$

where

$$\omega_\pm=\sqrt{\frac{\omega_c^{*2}}{2}+\tilde{\omega}_0^2\pm\sqrt{\frac{\omega_c^{*4}}{4}+\omega_c^{*2}\tilde{\omega}_0^2+\frac{\Delta^2}{4}+C_{12}^2}},\tag{4}$$

$$=\sqrt{\left[\frac{1}{2}\sqrt{\omega_c^{*2}+4\tilde{\omega}_0^2+\frac{(\Delta^2+4C_{12}^2)}{\omega_c^{*2}}}\pm\frac{\omega_c^*}{2}\right]^2-\frac{(\Delta^2+4C_{12}^2)}{4\omega_c^{*2}}},\tag{5}$$

$$\tilde{\omega}_0^2=\frac{1}{2}(C_{11}+C_{22});\quad \Delta=C_{11}-C_{22}\tag{6}$$

and $\omega_c^*=B/m^*c$ is the cyclotron frequency with the effective mass. (The results for the special case $C_{12}=0$ can also be found in Ref. 5.) The optical selection rules are the same as in the circular case, i.e., there are two possible types of excitations:

$$(\Delta n_+=\pm1 \text{ and } \Delta n_-=0)\quad \text{or}\quad (\Delta n_-=\pm1 \text{ and } \Delta n_+=0)\tag{7}$$

leading to the excitation energies $\Delta E=\omega_+$ and ω_-. It is easily seen that the form (5) reduces to the familiar formula in the circular case, where $\Delta=0$ and $C_{12}=0$. By inspection of Eq. (4) we find that a *soft mode* $\omega_-(B)=0$ can only occur if $C_{11}\cdot C_{22}=C_{12}^2$. For a diagonal $\mathbf{C}$ this means that $\min(C_{11},C_{22})=0$. The last condition is of importance for interacting dots considered in the next sections.

In the limiting case $B=0$ we obtain from Eq. (4)

$$\omega_\pm(B=0)=\sqrt{\frac{(C_{11}+C_{22})}{2}\pm\sqrt{\frac{(C_{11}-C_{22})^2}{4}+C_{12}^2}}.\tag{8}$$

We see that *degeneracy* $\omega_+(B=0)=\omega_-(B=0)$ can only happen if $C_{12}=0$ *and* $C_{11}=C_{22}$. For a diagonal confinement tensor with $C_{12}=0$ we obtain $\omega_+(B=0)=\max(\omega_1,\omega_2)$ and $\omega_-(B=0)=\min(\omega_1,\omega_2)$. As to be expected, we observe a gap between the two excitation curves $\omega_+(B)$ and $\omega_-(B)$ at $B=0$, if the two confinement frequencies do not agree.

Alternatively we can introduce the quantum numbers

$$k=\frac{(n_++n_-)-|n_+-n_-|}{2};\quad m_z=n_+-n_-,\tag{9}$$

where k is the node number and m_z turns in the circular limit into the angular momentum quantum number.

For arbitrary N, the center of mass (c.m.) $\mathbf{R}=(1/N)\Sigma_i\mathbf{r}_i$ can be separated $H=H_{c.m.}+H_{rel.}$ with

$$H_{c.m.}=\frac{1}{N}\left\{\frac{1}{2m^*}\left[\mathbf{P}+\frac{N}{c}\mathbf{A}(\mathbf{R})\right]^2+\frac{N^2}{2}\mathbf{R}\cdot\mathbf{C}\cdot\mathbf{R}\right\},\tag{10}$$

where $\mathbf{P}=-i\nabla_{\mathbf{R}}$ (see the Appendix). As well known, $H_{c.m.}$ does not contain the electron-electron interaction. $H_{c.m.}$ can be obtained from the one-electron Hamiltonian (2) by the substitution: $B\to NB$, $\mathbf{C}\to N^2\mathbf{C}$ and $H\to(1/N)H$. If we make the same substitution in the eigenvalues (3), we obtain

$$E_{c.m.}(n_+,n_-)=E_{N=1}(n_+,n_-),$$

i.e., the eigenvalues of the c.m. Hamiltonian are independent of N. In other words, in H there are excitations, in which the pair-correlation function is not changed, or classically speaking, where the charge distribution oscillates rigidly. Because

far-infrared (FIR) radiation (in the limit $\lambda \to \infty$) can excite only the c.m. subspace, all we see in FIR spectra is the c.m. modes.

III. DOT DIMER

We consider two *identical* elliptical dots centered at $\mathbf{a}_1 = (-a/2,0)$ and $\mathbf{a}_2 = (+a/2,0)$. We expand the Coulomb interaction between electrons in *different* dots in a multipole series and restrict ourselves to the dipole approximation. By introduction of c.m. and relative coordinates within each dot, the c.m. coordinates and the relative coordinates decouple (the tilde indicates that in this preliminary Hamiltonian a common gauge center for both dots is used):

$$\tilde{H} = \tilde{H}_{c.m.}(\mathbf{R}_1, \mathbf{R}_2) + \sum_{\alpha}^{1,2} \tilde{H}_{\alpha}(\{\mathbf{r}\}_{\alpha}^{(N-1)}). \tag{11}$$

$\{\mathbf{r}\}_{\alpha}^{(N-1)}$ symbolizes $(N-1)$ relative coordinates in the αth dot. This means, we have three decoupled Hamiltonians: the c.m. Hamiltonian and two Hamiltonians in the relative coordinates of either dot. This leads to two types of excitations:

(i) *Collective excitations* from $\tilde{H}_{c.m.}$ which involve the c.m. coordinates of both dots simultaneously. Because of the harmonic form (in the dipole approximation), there are exactly two modes per dot, thus a total of four. Each excitation can be classically visualized as vibrations of rigidly moving charge distributions of both dots.

(ii) *Intradot excitations* which are doubly degenerate for two identical dots. Because $\tilde{H}_{\alpha}(\{\mathbf{r}\}_{\alpha}^{(N-1)})$ is not harmonic (it includes the exact Coulomb interaction between the electrons within each dot, which is not harmonic), this spectrum is very complex. It is the excitation spectrum of a single dot *in a modified confinement potential* where the c.m. coordinate is fixed. The extra term in the modified confinement potential comes from the dipole contribution of the interdot Coulomb interaction.

In this section we consider only the c.m. Hamiltonian and focus our attention to the the effects of ellipticity in the dot confinement potential. The relative Hamiltonian for $N=2$ is explicitly given in the last section and solved for circular dots. For the elliptical confinement potential considered in this section, the relative Hamiltonian cannot be solved easily, even if we restrict ourselves to $N=2$, because the elliptic confinement potential breaks the circular symmetry of the rest of the relative Hamiltonian.

A. Center-of-mass Hamiltonian of the dimer

The c.m. Hamiltonian in the dipole approximation reads

$$\tilde{H}_{c.m.} = \frac{1}{N}\left\{ \sum_{\alpha}^{1,2} \frac{1}{2m^*}\left[\mathbf{P}_{\alpha} + \frac{N}{c}\mathbf{A}(\mathbf{U}_{\alpha} + \mathbf{a}_{\alpha}) \right]^2 + \frac{N^2}{2} \sum_{\alpha,\alpha'} \mathbf{U}_{\alpha} \cdot \mathbf{C}_{\alpha,\alpha'} \cdot \mathbf{U}_{\alpha'} \right\} \tag{12}$$

where the small elongation $\mathbf{U}_{\alpha}$ is defined by $\mathbf{R}_{\alpha} = \mathbf{a}_{\alpha} + \mathbf{U}_{\alpha}$ and $\mathbf{P} = -i\nabla_{\mathbf{R}} = -i\nabla_{\mathbf{U}}$. The tensor $\mathbf{C}$ is

$$C_{\alpha,\alpha} = \mathbf{\Omega} + \beta N \sum_{\alpha'(\neq\alpha)} \mathbf{T}(\mathbf{a}_{\alpha,\alpha'}), \tag{13}$$

$$C_{\alpha,\alpha'} = -\beta N \mathbf{T}(\mathbf{a}_{\alpha,\alpha'}) \quad \text{for} \quad \alpha \neq \alpha', \tag{14}$$

where $\mathbf{a}_{\alpha,\alpha'} = \mathbf{a}_{\alpha} - \mathbf{a}_{\alpha'}$, and the dipole tensor is

$$\mathbf{T}(\mathbf{a}) = \frac{1}{a^5}[3\mathbf{a}\circ\mathbf{a} - a^2\mathbf{I}] \tag{15}$$

containing a dyad product ($\circ$) and the unit tensor $\mathbf{I}$. As in the c.m. system of a single dot, the explicit N dependence in Eq. (12) cancels in the eigenvalues. What is left is only the N dependence in the dipole contribution of the dot interaction appearing in Eqs. (13) and (14). This means that the c.m. spectrum of interacting dots is no longer independent of N.

The term $\mathbf{a}_{\alpha}$ in the argument of the vector potential in Eq. (12) causes trouble in finding the eigenvalues. This shift is a consequence of the fact that we have to adopt a common gauge center for both dots (we chose the middle between both dots). This problem can be solved by applying the following unitary transformation:

$$H_{c.m.} = Q^{-1}\tilde{H}_{c.m.}Q; \quad Q = \prod_{\alpha}^{1,2} Q = e^{-\frac{1}{2}\frac{N}{c}(\mathbf{B}\times\mathbf{a}_{\alpha})\cdot\mathbf{U}_{\alpha}}. \tag{16}$$

In other words, $H_{c.m.}$ agrees with $\tilde{H}_{c.m.}$ except for the missing shift in the argument of the vector potential.

The four modes inherent in $H_{c.m.}$ are not yet explicitly known, because the four degrees of freedom are coupled. Decoupling into two oscillator problems of type (2) can be achieved by the following transformation:

$$\mathbf{U}^{(+)} = \frac{1}{2}(\mathbf{U}_2 + \mathbf{U}_1); \quad \mathbf{U}^{(-)} = \mathbf{U}_2 - \mathbf{U}_1. \tag{17}$$

This results in

$$H_{c.m.} = \frac{1}{2}H^{(+)} + 2H^{(-)}, \tag{18}$$

where

$$H^{(+)} = \frac{1}{N}\left\{ \frac{1}{2m^*}\left[\mathbf{P}^{(+)} + \frac{2N}{c}\mathbf{A}(\mathbf{U}^{(+)}) \right]^2 + \frac{N^2}{2}\mathbf{U}^{(+)}\cdot(4\mathbf{\Omega})\cdot\mathbf{U}^{(+)} \right\}, \tag{19}$$

$$H^{(-)} = \frac{1}{N}\left\{ \frac{1}{2m^*}\left[\mathbf{P}^{(-)} + \frac{N}{2c}\mathbf{A}(\mathbf{U}^{(-)}) \right]^2 + \frac{N^2}{2}\mathbf{U}^{(-)}\cdot\left(\frac{1}{4}\mathbf{\Omega} + \frac{N}{2}\beta\mathbf{T}(\mathbf{a}) \right)\cdot\mathbf{U}^{(-)} \right\}, \tag{20}$$

and $\mathbf{a}$ is a vector pointing from one dot center to the other. Then $\mathbf{T}(\mathbf{a})$ has the following components:

$$T_{11} = \frac{2}{a^3}; \quad T_{22} = -\frac{1}{a^3}; \quad T_{12} = T_{21} = 0. \tag{21}$$

Now we assume that the principle axes of the confinement potentials are in x_1-x_2 direction. This means

$$\Omega_{11}=\omega_1^2; \quad \Omega_{22}=\omega_2^2; \quad \Omega_{12}=\Omega_{21}=0. \tag{22}$$

The eigenvalues of $H^{(+)}$ can be obtained from Eqs. (3) and (4) with

$$\tilde{\omega}_0^2=\frac{1}{2}(\omega_1^2+\omega_2^2); \quad \Delta=(\omega_1^2-\omega_2^2) \tag{23}$$

and for $H^{(-)}$ with

$$\tilde{\omega}_0^2=\frac{1}{2}(\omega_1^2+\omega_2^2)+\frac{1}{2}p; \quad \Delta=(\omega_1^2-\omega_2^2)+3p, \tag{24}$$

where the interaction parameter is defined by

$$p=\frac{2N\beta}{a^3}. \tag{25}$$

Observe that the dependence on N cancels, except that included in p [see discussion following Eq. (10)]. It is important that the dot interaction influences the result only through a single parameter. This conclusion agrees with the semiphenomenological theory in Ref. 2.

In all our figures we express frequencies in units of the average confinement frequency $\omega_0=\frac{1}{2}(\omega_1+\omega_2)$, and Δ and p in units ω_0^2. Then, all systems can be characterized by the two parameters: ω_1/ω_2 and p. In other words, all systems having the ω_1/ω_2 ratio indicated in the figures are represented by the family of curves with the p values shown. The only exception we made is the cyclotron frequency ω_c^*. ω_c^*/ω_0 would be a good parameter in this sense, but we chose to use the magnetic field in T instead for better physical intuition. The conversion between both scales is given by $\omega_c^*[\text{a.u.}^*]=[(0.9134\times10^{-2})/m^*]B[\text{T}]$ or, $\omega_c^*[\omega_0]=\{(0.9134\times10^{-2})/m^*\omega_0[\text{a.u.}^*]\}B[\text{T}]$. In this paper we used $\omega_0=0.2$ a.u.$^*=2.53$ meV and m^* of GaAs. (We want to stress that this choice effects only the magnetic-field scale and not the qualitative features of the figures.) For easy comparison with experimental parameters we add the definition of effective atomic units (a.u.*) in GaAs ($m^*=0.067, \beta=1/12$) for the energy: 1 a.u.$^*=4.65\times10^{-4}$ double Rydberg$=12.64$ meV, and for the length: 1 a.u.$^*=1.791\times10^2$ bohrs$=0.9477\times10^2$ Å.

Because $\mathbf{U}^{(+)}$ agrees with the *total* c.m. $\mathbf{R}=\frac{1}{2}(\mathbf{R}_1+\mathbf{R}_2)$ of the system, $H^{(+)}$ is the total c.m. Hamiltonian. For $B=0$, the eigenmodes can be visualized by classical oscillations. The two eigenmodes of $H^{(+)}$ are (rigid) in-phase oscillations of the dots in x_1 and x_2 direction, respectively. Because of the Kohn theorem (see the Appendix), the independence of $H^{(+)}$ on the Coulomb interaction does not only hold in the dipole approximation, but it is rigorous. This shows also that the dipole approximation is consistent with the Kohn theorem, which is not guaranteed for single-particle approaches. Because FIR radiation excites (in the dipole approximation) only the c.m. modes, it is only the p-independent eigenmodes of $H^{(+)}$ which are seen in FIR absorption experiments.

This statement is in contradiction to Ref. 4. They performed numerical diagonalizations for a lateral pair of circular dots confining the set of basis functions to the lowest Landau level and considering parallel spin configurations only. This is justified in the limit of high magnetic fields. They found a splitting of the two dipole allowed modes at $B=0$ due to dot interaction and some anticrossing structures in the upper mode, whereas the lower mode is always close to the single-particle mode. This fact is already a strong indication that the missing higher Landau levels cause both spurious effects. (Observe that the lifting of the degeneracy at $B=0$ in the dipole allowed excitations in Fig. 1 is due to the ellipticity of the intrinsic confinement and not due to dot interaction.)

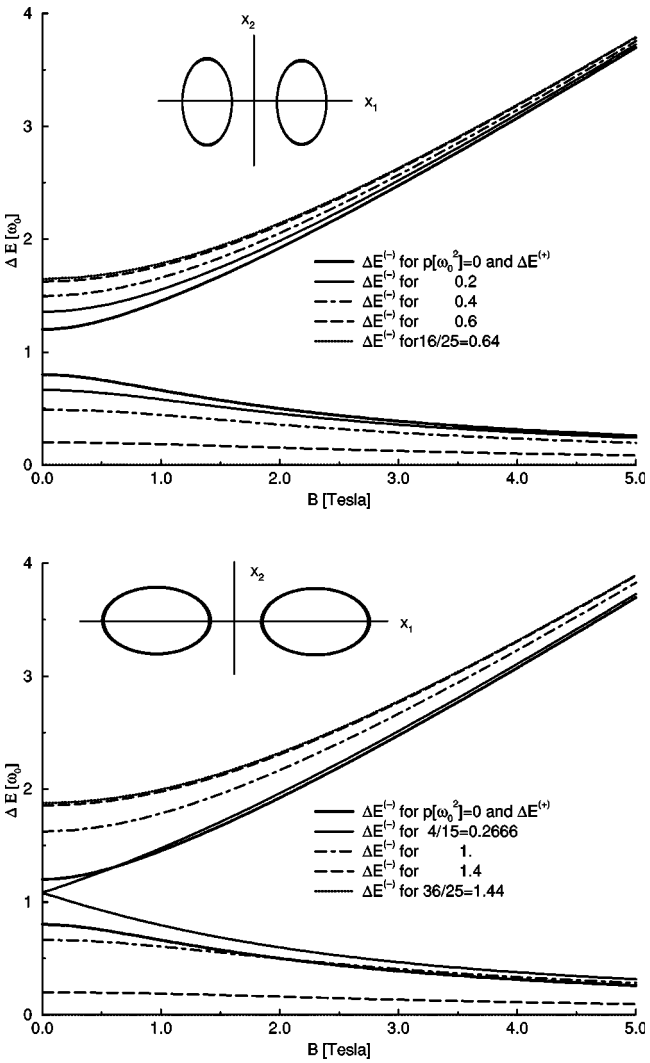

FIG. 1. Excitation energies $\Delta E_{\pm}^{(\pm)}=\omega_{\pm}^{(\pm)}$ for a dimer of elliptical dots as a function of the magnetic field for some discrete values of the interaction parameter p (p values in the inset are in units ω_0^2). The ratio of the oscillator frequencies in the direction of the capital axes ω_1/ω_2 is (a) 3/2 and (b) 2/3. The dipole allowed excitations $\Delta E^{(+)}$ of $H^{(+)}$ (thick full line) are not influenced by the dot interaction and therefore independent of p.

The eigenvalues of $H^{(-)}$ do depend on p because the dots oscillate (rigidly) in its two eigenmodes in opposite phase, one mode in x_1 and one mode in x_2 direction. This leads to a change in the Coulomb energy. The two eigenmodes of $H^{(-)}$ can also be described as a breathing mode (in x_1 direction) and a shear mode (in x_2 direction).

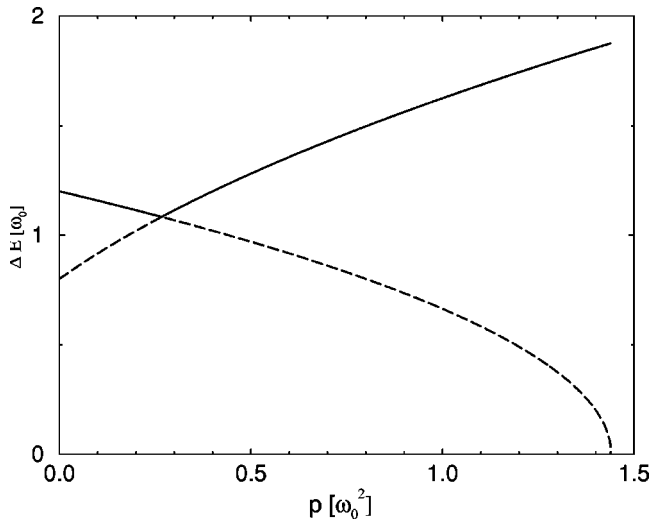

FIG. 2. Excitation energies $\Delta E_{\pm}^{(-)}=\omega_{\pm}^{(-)}$ of the Hamiltonian $H^{(-)}$ for $B=0$ and $\omega_1/\omega_2=2/3$ as a function of the interaction parameter p.

B. Special features of the excitation spectrum

In Figs. 1(a) and (b) the four excitation frequencies of the dimer are shown with p as a parameter. For $p=0$, the two modes $\omega_{\pm}^{(-)}$ agree with the two modes $\omega_{\pm}^{(+)}$. In all symbols, the superscript sign refers to the system $H^{(+)}$ and $H^{(-)}$ (c.m. or relative coordinate), and the subscript sign discriminates the two modes of the same system. The two modes $\omega_{\pm}^{(+)}$ are independent of p. There are two qualitatively different cases. (Consider that ω_1 is the oscillator frequency parallel to the line, which connects the two dot centers, and ω_2 is the oscillator frequency perpendicular to this line.) If $\omega_1 \geqslant \omega_2$ [Fig. 1(a), the gap between $\omega_{+}^{(-)}$ and $\omega_{-}^{(-)}$ at $B=0$ increases steadily with increasing p until, for a critical $p_{cr}=\omega_2^2$ (in our numerical case: $p_{cr}[\omega_0^2]=16/25=0.64$) the lower mode $\omega_{-}^{(-)}$ becomes soft. This transition is *independent* of B. For $\omega_1 \leqslant \omega_2$ the gap between $\omega_{+}^{(-)}$ and $\omega_{-}^{(-)}$ at $B=0$ first decreases with increasing p until it vanishes for $p=\frac{1}{3}(\omega_2^2-\omega_1^2)$ (in our numerical case: $p[\omega_0^2]=4/15=0.27$). Afterwards, it increases until the lattice becomes soft at $p_{cr}=\omega_2^2$ (in our numerical case: $p_{cr}[\omega_0^2]=36/25=1.44$). The dependence of the two excitation energies $\omega_{+}^{(-)}$ and $\omega_{-}^{(-)}$ on p for $B=0$ in the second case is shown in Fig. 2. Comparison of Figs. 2(a) and (b) demonstrates that the dot architecture in Fig. 2(a) is much more sensitive to interdot interaction than that in Fig. 2(b). Thus, if we want to observe or use the instability, this event happens in case 2(a) for for smaller p (or larger lattice constants) than in case 2(b). Additionally, the assumption of nonoverlapping dot wave functions (for a given lattice constant) is better fulfilled in case 2(a) than in case 2(b).

For GaAs as a typical substance, Eq. (25) can be rewritten in more convenient units as

$$p[\omega_0^2]=\frac{2.26\times 10^7 N}{(a[\text{Å}])^3(\omega_0[\text{meV}])^2}. \tag{26}$$

Obviously, we need large dots (large N, small ω_0, which means large polarizability), and a small dot distance a for a seizable interaction effect. On the other hand, the dot radius for $N=1$ is of order of the effective magnetic length[1] $l_0=[(2\omega_0)^2+(\omega_c^*)^2]^{-1/4}$, which reads for GaAs

$$l_0[\text{Å}]=\frac{238}{\{(\omega_0[\text{meV}])^2+0.739(B[\text{T}])^2\}^{1/4}} \tag{27}$$

and we need small dots and high magnetic fields for small overlap. Consequently, a magnetic field helps avoiding overlap of the dots, although, e.g., the critical p for soft modes is independent of B. The question is whether there exists a window between these two (partly) conflicting demands. For an order-of-maigntude estimate, let us consider GaAs with ω_0 as chosen above and the worst case $N=1$. Then Eq. (26) with a typical $p[\omega_0^2]=0.1$ (which seems to be the minimum for any observable effect) provides a dot distance of $a[\text{Å}]=327$ and Eq. (27) gives for $B=0$ a radius of $l_0[\text{Å}]=150$ and for $B[\text{T}]=10$ a radius of $l_0[\text{Å}]=80$. Consequently, the constraint $l_0<a/2$ for our model can be fulfilled. For obtaining larger interaction effects the parameters have to be optimized.

The next question is what happens in *mode softening* physically? First, it is the antisymmetric shear mode $\omega_{-}^{(-)}$ which has the lowest frequency and which becomes soft. If the interaction parameter is strong enough ($p>p_{cr}$), the *decrease* in interdot-Coulomb energy with increasing elongation of the dots becomes larger than the *increase* of confinement potential energy. Because *in the harmonic model* both energies depend quadratically on elongation, the dimer *would* be ionized, i.e., stripped of the electrons. Clearly, in this case we have to go beyond the dipole approximation for the interdot interaction and beyond the harmonic approximation for the confinement potential.

In order to obtain a hand-waving picture of what happens, the confinement potential of the system for shear mode oscillations is supplemented by a fourth-order term in the following way: $V_{conf.}=2N[\frac{1}{2}\omega_2^2U^2-AU^4]$ with $(A>0)$, and the Coulomb interaction in fourth order reads: $V_{int}=-pNU^2+(3pN/a^2)U^4$ where $p=2N\beta/a^3$ as above. Then, the stability condition reads

$$\frac{V_{tot}}{N}=(\omega_2^2-p)U^2+\left(\frac{3p}{a^2}-2A\right)U^4\geqslant 0. \tag{28}$$

The condition for the existence of a bound state is that the U^4 term is positive: $3p/a^2>2A$. For a positive U^2 term ($p<\omega_2^2$), the equilibrium position is $U_0=0$. If the U^2 term becomes negative ($p>\omega_2^2$), the system finds a new equilibrium at a finite elongation

$$U_0=\pm\sqrt{\frac{(p-\omega_2^2)}{2(3p/a^2-2A)}}. \tag{29}$$

This new ground state is doubly degenerate: $\mathbf{U}_1=(-a,+U_0)$, $\mathbf{U}_2=(+a,-U_0)$ and $\mathbf{U}_1=(-a,-U_0)$, $\mathbf{U}_2=(+a,+U_0)$ have the same energy. In short, at $p_{cr}=\omega_2^2$ there is an electronic phase transition to a polarized state, where the equilibrium position of the c.m. is no more in the middle of the dots. At the end we want to stress that all these stability considerations are only valid if the confinement potential is

not changed under elongation of the c.m. of the dots. Second, it is not rigorous to include the fourth-order terms *after* separation of c.m. and relative coordinates, because in fourth order these two coordinates do not decouple exactly.

IV. DOT LATTICE

We consider a periodic lattice of *equal* quantum dots at lattice sites $\mathbf{R}^{(0)}_{n,\alpha}=\mathbf{R}^{(0)}_n+\mathbf{a}_\alpha$. The vectors $\mathbf{R}^{(0)}_n$ form a Bravais lattice and $\mathbf{a}_\alpha$ runs over all sites within an unit cell. In developing a theory for these lattices we have to repeat all steps in Sec. II from Egs. (11) to (16) just by supplementing the index α by the index n for the unit cell.

A. Center-of-mass Hamiltonian of the dot lattice

The c.m. Hamiltonian in the dipole approximation then reads

$$H_{c.m.}=\frac{1}{N}\left\{\sum_{n,\alpha}\frac{1}{2m^*}\left[\mathbf{P}_{n,\alpha}+\frac{N}{c}\mathbf{A}(\mathbf{U}_{n,\alpha})\right]^2+\frac{N^2}{2}\sum_{\substack{n,\alpha\\ n',\alpha'}}\mathbf{U}_{n,\alpha}\cdot\mathbf{C}_{n,\alpha;n',\alpha'}\cdot\mathbf{U}_{n',\alpha'}\right\},\tag{30}$$

where $\mathbf{U}_{n,\alpha}=\mathbf{R}_{n,\alpha}-\mathbf{R}^{(0)}_{n,\alpha}$ is the elongation of the c.m. at lattice site (n,α) and the force constant tensor $\mathbf{C}$ is defined in analogy to Eqs. (13) and (14).

The Hamiltonian (30) is a phonon Hamiltonian in an additional homogeneous magnetic field. The first stage of decoupling can be achieved by the usual phonon transformation

$$\mathbf{U}_{n,\alpha}=\frac{1}{\sqrt{N_c}}\sum_{\mathbf{q}}^{BZ}e^{-i\mathbf{q}\cdot R^{(0)}_n}\mathbf{U}_{\mathbf{q},\alpha},\tag{31}$$

$$\mathbf{P}_{n,\alpha}=\frac{1}{\sqrt{N_c}}\sum_{\mathbf{q}}^{BZ}e^{+i\mathbf{q}\cdot R^{(0)}_n}\mathbf{P}_{\mathbf{q},\alpha},\tag{32}$$

where N_c is the number of unit cells and the transformed coordinates have the following properties: $\mathbf{U}_{-\mathbf{q},\alpha}=\mathbf{U}^*_{\mathbf{q},\alpha}=\mathbf{U}^\dagger_{\mathbf{q},\alpha}$ and $\mathbf{P}_{-\mathbf{q},\alpha}=\mathbf{P}^\dagger_{\mathbf{q},\alpha}$. The Hamiltonian in the new coordinates is a sum of N_c subsystems of dimension $2\times$ number of dots per unit cell: $H_{c.m.}=\Sigma_{\mathbf{q}}H_{\mathbf{q}}$, where

$$H_{\mathbf{q}}=\frac{1}{N}\left\{\sum_{\alpha}\frac{1}{2m^*}\left[\mathbf{P}_{\mathbf{q},\alpha}+\frac{N}{c}\mathbf{A}(\mathbf{U}^*_{\mathbf{q},\alpha})\right]^\dagger\cdot\left[\mathbf{P}_{\mathbf{q},\alpha}+\frac{N}{c}\mathbf{A}(\mathbf{U}^*_{\mathbf{q},\alpha})\right]+\frac{N^2}{2}\sum_{\alpha,\alpha'}\mathbf{U}^*_{\mathbf{q},\alpha}\cdot\mathbf{C}_{\mathbf{q};\alpha,\alpha'}\cdot\mathbf{U}_{\mathbf{q},\alpha'}\right\}.\tag{33}$$

The dynamical matrix is defined by

$$\mathbf{C}_{\mathbf{q};\alpha,\alpha'}=\sum_n e^{i\mathbf{q}\cdot\mathbf{R}^{(0)}_n}\mathbf{C}_{\alpha,\alpha'}(\mathbf{R}^{(0)}_n);\quad \mathbf{C}_{\alpha,\alpha'}(\mathbf{R}^{(0)}_n)=\mathbf{C}_{n,\alpha;0,\alpha'}\tag{34}$$

and it is Hermitean $\mathbf{C}_{\mathbf{q};\alpha',\alpha}=\mathbf{C}^*_{\mathbf{q};\alpha,\alpha'}=\mathbf{C}_{-\mathbf{q};\alpha,\alpha'}$.

Next we want to recover the limiting case considered in Sec. III. If the dots in a given unit cell are far away from those in neighboring cells, then in Eq. (34) only the term with $\mathbf{R}^{(0)}_n=0$ contributes, $\mathbf{C}$ does not depend on $\mathbf{q}$, consequently the index $\mathbf{q}$ is redundant, and Eq. (33) agrees with Eq. (12).

Our preliminary result (33) is not yet diagonal in α,α'. In some special cases (see, e.g., two identical dots per unit cell considered in Sec. III) this can be achieved by an unitary transformation

$$\mathbf{U}_{\mathbf{q},\alpha}=\sum_{\alpha'}Q_{\mathbf{q};\alpha,\alpha'}\cdot\tilde{\mathbf{U}}_{\mathbf{q},\alpha'};\quad Q^*_{\mathbf{q};\alpha',\alpha}=Q^{-1}_{\mathbf{q};\alpha,\alpha'}\tag{35}$$

under which the one-particle term in Eq. (33) is invariant and the transformed interaction term

$$\frac{1}{2}\sum_{\alpha,\alpha'}\tilde{\mathbf{U}}^*_{\mathbf{q},\alpha}\cdot\tilde{\mathbf{C}}_{\mathbf{q};\alpha,\alpha'}\cdot\tilde{\mathbf{U}}_{\mathbf{q},\alpha'}\quad\text{with}$$

$$\tilde{\mathbf{C}}_{\mathbf{q};\alpha,\alpha'}=\sum_{\alpha_1,\alpha_2}Q^{-1}_{\alpha,\alpha_1}\mathbf{C}_{\mathbf{q};\alpha_1,\alpha_2}Q_{\alpha_2,\alpha'}\tag{36}$$

can be made diagonal $\tilde{\mathbf{C}}_{\mathbf{q};\alpha,\alpha'}=\tilde{\mathbf{C}}_{\mathbf{q};\alpha}\delta_{\alpha,\alpha'}$ by a proper choice of $Q_{\alpha,\alpha'}$. Now, Eq. (33) reads $H_{\mathbf{q}}=\Sigma_\alpha H_{\mathbf{q},\alpha}$, where

$$H_{\mathbf{q},\alpha}=\frac{1}{N}\left\{\frac{1}{2m^*}\left[\tilde{\mathbf{P}}_{\mathbf{q},\alpha}+\frac{N}{c}\mathbf{A}(\tilde{\mathbf{U}}^*_{\mathbf{q},\alpha})\right]^\dagger\cdot\left[\tilde{\mathbf{P}}_{\mathbf{q},\alpha}+\frac{N}{c}\mathbf{A}(\tilde{\mathbf{U}}^*_{\mathbf{q},\alpha})\right]+\frac{N^2}{2}\tilde{\mathbf{U}}^*_{\mathbf{q},\alpha}\cdot\tilde{\mathbf{C}}_{\mathbf{q};\alpha}\cdot\tilde{\mathbf{U}}_{\mathbf{q},\alpha}\right\}.\tag{37}$$

The eigenvalues of Eq. (37) can be obtained from those of Eq. (2) because corresponding quantities have the same commutation rules. Such an unitary transformation does not exist, e.g., for two different dots per cell (see Ref. 12). Then Eq. (33) has to be solved directly using the method described in Ref. 6.

B. Dynamical matrix for Bravais lattices

From now on we consider *Bravais lattices* what means that we can forget the indices α in the first part of this section. Then the dynamical matrix

$$\mathbf{C}_{\mathbf{q}}=\mathbf{\Omega}+\beta N\sum_{\mathbf{R}^{(0)}_n\neq 0}(1-e^{i\mathbf{q}\cdot\mathbf{R}^{(0)}_n})\mathbf{T}(\mathbf{R}^{(0)}_n)\tag{38}$$

is real and symmetric, but generally not diagonal, even if $\mathbf{\Omega}$ is diagonal. A very important conclusion is apparent in Eq. (38). *In the limit* $\mathbf{q}\to 0$, *the interdot interaction* (*represented by* β) *has no influence on* $\mathbf{C}_{\mathbf{q}}$ *and therefore on the spectrum. This means that the excitation spectrum observed by FIR spectroscopy is not influenced by interdot interaction and agrees with the one-electron result (as in the single dot).* This statement is rigorous for parabolic confinement (see the Appendix). It can also be understood intuitively, because a $q=0$ excitation is connected with homogeneous in-phase elongations of the dots which do not change the distance between the electrons. We want to mention that this conclusion seems to be in contradiction with the experimental work in Ref. 11. They found a splitting of the upper and lower

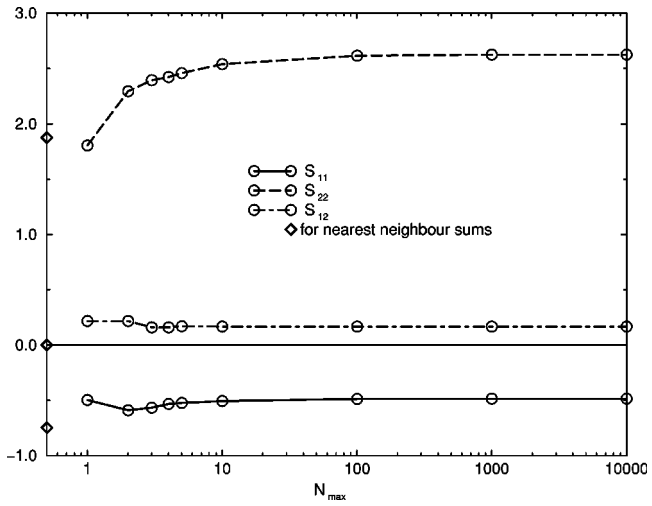

FIG. 3. Convergency of the lattice sums S_{ik} as defined in Eq. (41) with increasing number of cubic shells N_{max} for $\mathbf{q}$ in the middle of the irreducible Brillouin zone.

excitation branch at $B=0$ and $q=0$ for circular dots in a rectangular lattice, which they interpreted within a phenomenological model of interacting dipoles as a consequence of lattice interaction. However, they use mesoscopic dots with a diameter of 370 000 Å and lattice periods of 400 000 and 800 000 Å. These dots are clearly beyond our microscopic quantum mechanical model, which rests on a parabolic confinement.

For the *rectangular lattices* considered in our numerical examples we define $\mathbf{R}^{(0)}=N_1a_1\mathbf{e}_1+N_2a_2\mathbf{e}_2$ and $\mathbf{q}=q_1(2\pi/a_1)\mathbf{e}_1+q_2(2\pi/a_2)\mathbf{e}_2$ with the lattice constants a_1 and a_2 and integers N_1 and N_2 characterizing the lattice sites. The components of $\mathbf{q}$ vary in the Brillouin zone (BZ) in the range $[-1/2,+1/2]$. The dipole tensor (15) reads

$$\mathbf{T}(N_1,N_2)=\frac{1}{(N_1^2a_1^2+N_2^2a_2^2)^{5/2}}\times\begin{bmatrix}(2N_1^2a_1^2-N_2^2a_2^2) & 3N_1N_2a_1a_2\\ 3N_1N_2a_1a_2 & (2N_2^2a_2^2-N_1^2a_1^2)\end{bmatrix}. \tag{39}$$

Although for all figures the exact dynamical matrix is used, it is useful to consider the results with *nearest-neighbor* (NN) lattice sums in Eq. (38) separately. This provides simple formulas for order-of-magnitude estimates.

$$C_{11}=\omega_1^2+2p_1[1-\cos(2\pi q_1)]-p_2[1-\cos(2\pi q_2)],$$

$$C_{22}=\omega_2^2+2p_2[1-\cos(2\pi q_2)]-p_1[1-\cos(2\pi q_1)],$$

$$C_{12}=\Omega_{12}, \tag{40}$$

where we introduced the interaction parameters $p_i=2\beta N/a_i^3$.

The convergence of the lattice sums S_{ik} in the dynamical matrix is shown Fig. 3. S_{ik} is defined by

$$C_{ik}=\Omega_{ik}+p_2S_{ik} \tag{41}$$

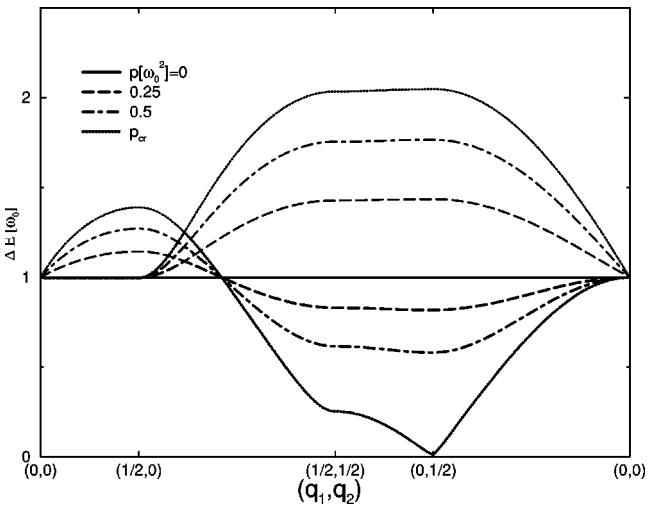

FIG. 4. Magnetophonon dispersion at $B=0$ for several interaction parameter values and $\mathbf{q}$ on symmetry lines of the Brillouin zone. ($p=p_2$ values in the inset are in units ω_0^2.) Thick (lower) and thin (upper) lines indicate ΔE_- and ΔE_+, respectively.

and depends only on $\mathbf{q}$ and the ratio a_1/a_2. Apart from the off-diagonal elements, which vanish in NN approximation, the error of the NN approximation is less than 30%.

C. Special features of the magnetophonon spectrum

Figs. 4–6 show the magnetophonon spectrum for circular dots on a rectangular lattice with $a_1=2a_2$. (The term *magnetophonon* is attributed to the fact that there is no exchange and there are harmonic forces between the oscillating individuals. One could also call them *magnetoplasmons*, if one wants to emphasize that it is only electrons which oscillate, and no nuclei) Because the two interaction parameters have a fixed ratio, it suffices to use one of them for characterizing the interaction strength. We chose the larger one $p_2=p$. For $B=0$ and isolated dots ($p=0$), the two excitation modes are degenerate. If we tune up the interaction strength represented by p, a $\mathbf{q}$-dependent splitting appears (see Fig. 4).

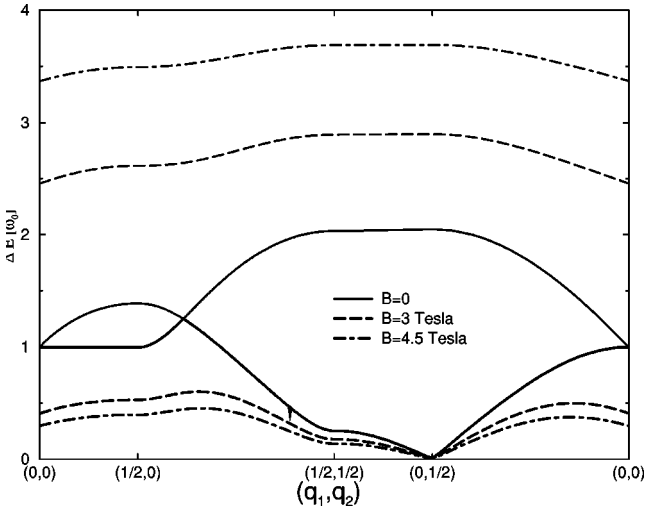

FIG. 5. The same as Fig. 4, but for $p=p_{cr}$ and several magnetic fields.

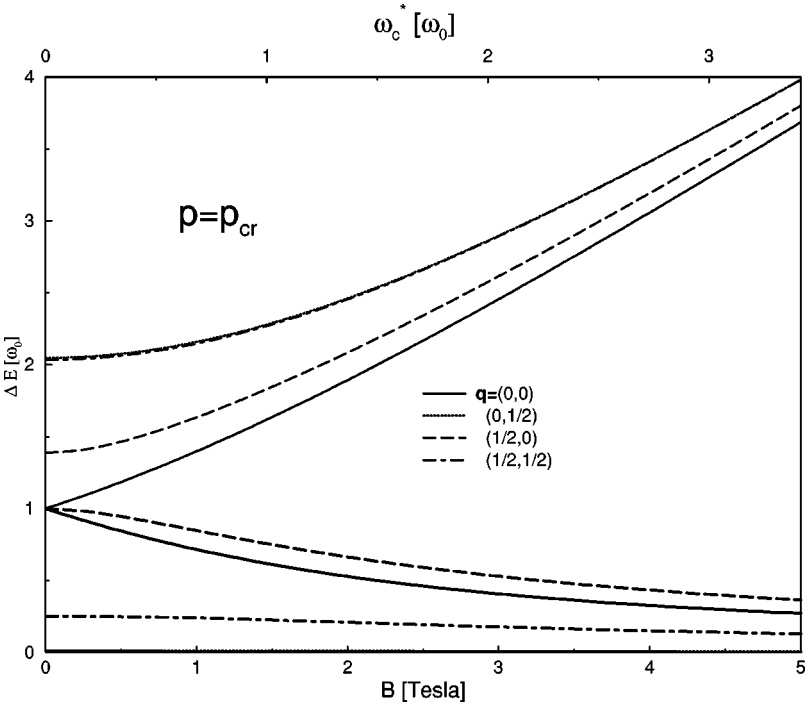

FIG. 6. Magnetophonon excitations as a function of B for the symmetry points in the Brillouin zone. The upper abscissa is independent of the effective mass, the lower one applies to GaAs.

This splitting is a manifestation of the dot interaction. For a certain critical p_{cr} the lower mode becomes soft. This feature will be discussed below. There are points in the BZ, however, where the *degeneracy* for finite p remains. These points will be investigated now. We demonstrated in Sec. II after formula (8) that *necessary* for degeneracy is $C_{12}=0$, i.e., the dynamical matrix must be diagonal. Then the points with degeneracy are defined by the condition $C_{11}=C_{22}$. As seen in Eq. (38), for circular dots $\omega_1=\omega_2=\omega_0$ this happens in the center of the BZ $\mathbf{q}=0$. The next question to be discussed is if there are other points with degeneracy. The first condition $C_{12}=0$, is fulfilled for all points on the surface of the BZ. The second condition must be investigated for special cases. We find that for quadratic lattices $a_1=a_2$ with circular dots $\omega_1=\omega_2$ both modes are degenerate at the point $\mathbf{q}=(1/2,1/2)$. In the case shown in Fig. 4 this point is somewhere between $(1/2,1/2)$ and $(1/2,0)$. In NN approximation (40), however, this equation is even fulfilled on full curves in the BZ defined by $p_1[1-\cos(2\pi q_1)]=p_2[1-\cos(2\pi q_2)]$. In a cubic lattice, this is the straight lines $q_2=\pm q_1$. The contributions beyond NNs remove the exact degeneracy on this curve in the interior of the BZ, but leave a kind of anticrossing behavior of the two branches.

An important parameter, which characterizes the influence of the dot interaction in circular dots, is the *bandwidth* at $B=0$, i.e., the maximum splitting of the two branches due to dot interaction. (Remember that this splitting vanishes for noninteracting circular dots.) Assume $a_1>a_2$. Then the largest splitting for circular dots in NN approximation appears at $\mathbf{q}=(0,1/2)$ and has the amount

$$W=\max(\Delta E_+-\Delta E_-)=\max(\omega_+-\omega_-)=\sqrt{\omega_0^2+4p_2}-\sqrt{\omega_0^2-2p_2}. \tag{42}$$

For small dot interaction and in units ω_0, this is proportional to the interaction parameter $W/\omega_0\to 3p_2$.

We next discuss the appearance of *soft modes*. The question is, for which $\mathbf{q}$, B and interaction parameter p this happens. The general condition for vanishing of the lowest mode is $C_{11}\cdot C_{22}=C_{12}^2$ (see Sec. II). In this condition the magnetic field does not appear. For circular dots and with the definition (41) this equation reads

$$[\omega_0^2+p_2S_{11}][\omega_0^2+p_2S_{11}]=p_2^2S_{12}^2. \tag{43}$$

After introducing a dimensionless critical interaction parameter $p[\omega_0^2]=p_2/\omega_0^2$, we obtain a quadratic equation for $p[{}^2_0]$ which has the solution

$$p[\omega_0^2]=-\frac{1}{2}\frac{\mathrm{Tr}}{\mathrm{Det}}\pm\sqrt{\left(\frac{1}{2}\frac{\mathrm{Tr}}{\mathrm{Det}}\right)^2-\frac{1}{\mathrm{Det}}}, \tag{44}$$

where $\mathrm{Det}=S_{11}S_{22}-S_{12}^2$ and $\mathrm{Tr}=S_{11}+S_{22}$. For our numerical case $a_1=2a_2$ and NN interaction for S_{ik} the lowest mode becomes soft at $\mathbf{q}=(0,1/2)$ and the critical interaction parameter is $p[\omega_0^2]=1/2$. Inclusion of lattice contributions beyond NN shifts $p[\omega_0^2]$ to 0.7543. The most important result of this paragraph is that lattice softening is *independent* of B (see also Figs. 5 and 6). The latter conclusion is *exact* within the range of validity of the Hamiltonian (30) and no consequence of any subsequent approximation or specialization.

V. INTRADOT EXCITATIONS FOR $N=2$

Intradot excitations for circular dots in a cubic lattice and for $N=2$ can be calculated easily. We define the relative coordinate $\mathbf{r}=\mathbf{r}_2-\mathbf{r}_1$, and assume that all dots are equivalent (also with respect to their environment). Then the indexes (n,α) can be chosen as $(0,0)$ and omitted. The relative Hamiltonian reads

$$H_{rel}=2\left\{\frac{1}{2m^*}\left[\mathbf{p}+\frac{1}{2c}\mathbf{A}(\mathbf{r})\right]^2+\frac{1}{2}\mathbf{r}\cdot\mathbf{D}\cdot\mathbf{r}+\frac{\beta}{2r}\right\}, \tag{45}$$

where $\mathbf{p}=-i\nabla_{\mathbf{r}}$ and

$$\mathbf{D}=\frac{1}{4}\mathbf{\Omega}+\frac{\beta}{2}\mathbf{T}_0;\quad \mathbf{T}_0=\sum_{n,\alpha(\neq 0,0)}\mathbf{T}(\mathbf{R}^{(0)}_{n,\alpha}). \tag{46}$$

It is worth emphasizing that H_{rel} contains a contribution from neighboring dots, originating from the interdot Coulomb interaction. A trivial angular dependent part can only be decoupled from H_{rel}, or, the two-dimensional Schrödinger equation can be traced back to an ordinary radial Schrödinger equation, if the term $\mathbf{r}\cdot\mathbf{D}\cdot\mathbf{r}$ has the same circular symmetry as the intradot Coulomb term $\beta/(2r)$. Therefore we confine ourselves to circular dots on a cubic lattice, and we have

$$\mathbf{T}_0=\frac{1}{a^3}\sum_{N_1,N_2\neq 0,0}\frac{1}{(N_1^2+N_2^2)^{3/2}}\mathbf{I}\approx\frac{4}{a^3}\mathbf{I}, \tag{47}$$

where the simple result is in NN approximation. Using the interaction parameter $p=2N\beta/a^3$ (with $N=2$) defined above, we obtain

$$\mathbf{D}=\frac{1}{4}(\omega_0^2+2p)\mathbf{I}. \tag{48}$$

In this way, dot interaction defines an effective confinement frequency $\omega_{0,eff}^2=\omega_0^2+2p$. This means that *the c.m. excitations have to be calculated (or interpreted) with another confinement potential then the relative excitations*. In our figures we present results for $\omega_{0,eff}=0.2$ a.u.*, which agrees with the bare confinement potential used in Sec. IV and the mean value in Sec. III. Because our results are presented in units of ω_0, they depend on ω_0 only weakly through the differing influence of electron-electron interaction. For the absolute values, however, the influence of the dot interaction can be tremendous.

In the relative motion there is a coupling between orbital and spin parts through the Pauli principle. For $N=2$ and a circular effective confinement, Pauli principle demands that orbital states with even and odd relative angular momentum m_i must be combined with singlet and triplet spin states, respectively (see, e.g., Ref. 7). For the c.m. motion there is no interrelation between orbital and spin part because the c.m. coordinate is fully symmetric with respect to particle exchange. Consequently, any c.m. wave function can be combined with a given spin eigenfunction. The only spin-dependent term in the total energy considered here is the *Zeeman term*, which reads in our units

$$\frac{E_B}{\omega_0}=0.9134\times 10^{-2}g_s\frac{B[\mathrm{T}]}{\omega_0[\mathrm{a.u.}^*]}\frac{M_s}{2}, \tag{49}$$

where we used $g_s=-0.44$ for the gyro-magnetic factor of GaAs from Ref. 8. The total spin quantum number is $M_s=0$ for the singlet state and $0,\pm 1$ for the triplet state. One of the most interesting points in quantum dot physics is that the total orbital angular momentum of the ground state depends on the magnetic field (see, e.g., Refs. 8 and 9). This feature is a consequence of electron-electron interaction. For our parameter values, the relative orbital angular momentum of the ground state m_i changes from 0 to -1, from -1 to -2, and from -2 to -3 at $B=1.250$, 4.018, and 5.005 T. This corresponds to a sequence $M_s=0,+1,0,+1$ for the spin quantum number. Figures 7(a)–(c) show the excitation frequencies for three B values lying within the first three regions. m_f is the relative orbital angular momentum of the final state.

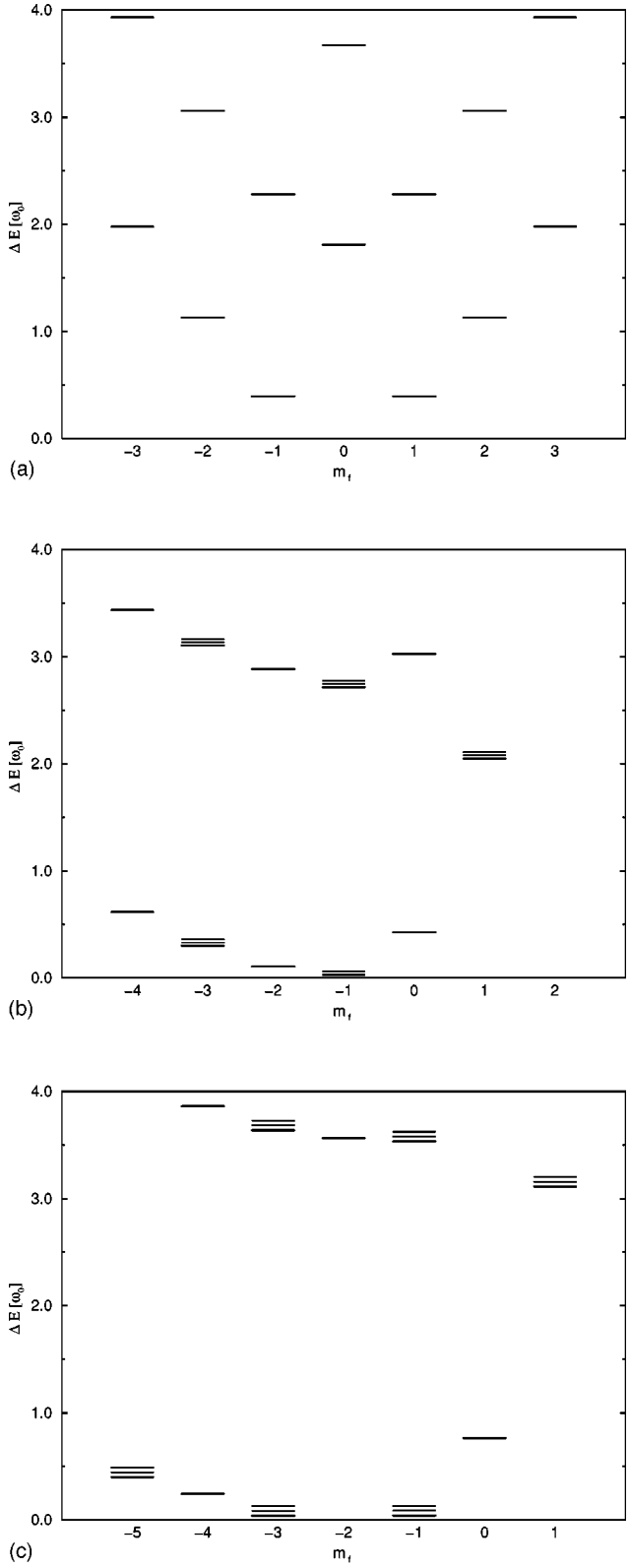

FIG. 7. Intradot excitation energies (in units of the *effective* confinement frequency) for $B=0$ (a), $B=3$ T (b), and $B=4.5$ T (c). The corresponding relative orbital angular momenta of the ground state are $m_i=0$ (a), -1 (b), and -2 (c) and the spin angular momenta $M_s=0$ (a), $+1$ (b), and 0 (c).

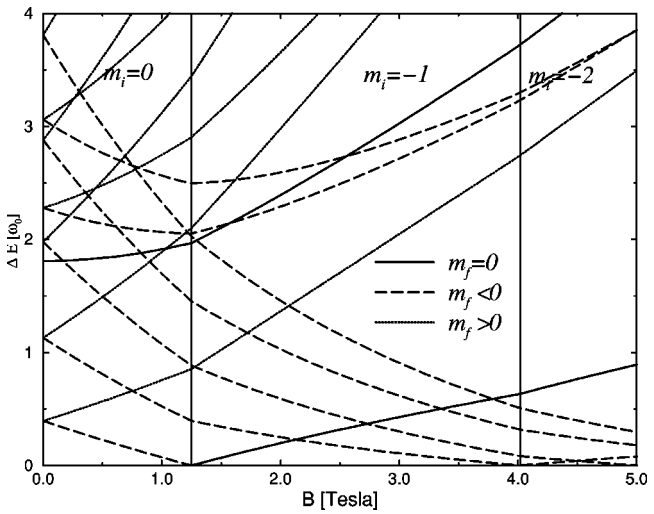

FIG. 8. Intradot excitation energies (in units of the *effective* confinement frequency) as a function of the magnetic field. The small Zeeman splitting is neglected. The B values, where the angular momenta of the ground-state change, are indicated by vertical lines. The absolute value of the final-state orbital momentum m_f of the curves at $B=0$ grows from bottom to top by 1 starting with 0.

All excitations are included irrespective of selection rules. For dipole transitions only two of them would remain (the lowest excitation with $m_f=m_i\pm1$). For $B=0$, the lowest excitation energy (in units ω_0) for noninteracting electrons would be 1. As seen in in Fig. 7(a), electron-electron interaction decreases this value by at least a factor of 1/2. The same holds qualitatively for finite B. This is connected to the fact, that the ground state depends on B. Let us consider an example. For $B=1.250$ T the ground state switches from $m_i=0$ to $m_i=-1$. This implies that for B approaching this transition field from below, the excitation energy for diole allowed transition from $m_i=0$ to $m_f=-1$ converges to 0. In other words, there is a level crossing at the the transition field. Therefore very small transition energies and switching of the ground state are connected.

For a qualitative understanding, Figs. 7(a)–(c) can be used together with Figs. 1(a), (b), 4, and 5 to investigate the relative position of collective and intradot excitations. The conclusion is that for small dot interaction (for p well below p_{cr}), the lowest intradot excitation energies lie well below the lowest c.m. excitations. Apart from using a different terminology, this conclusion agrees with the experimental findings in Ref. 10.

Figures 7(b) and (c), which belong to finite B, show the Zeeman splitting. All transition energies to final states with odd m_f are triplets because the corresponding spin state is a triplet state. The thin lines of a triplet belong to spin-flip transitions.

In Fig. 8 the B dependence of the lowest excitation energies is shown. It is clearly seen that the curves exhibit a kink at those B values, where the ground-state configuration changes. The size of the kink decreases with increasing B. If this kink could be resolved experimentally (e.g., by electronic Raman spectroscopy), it would be a direct indication for the change of the ground-state configuration, and thus an experimentally observable consequence of electron-electron interaction.

VI. SUMMARY

We solved the Schrödinger equation for a lattice of *identical* parabolic (but not necessarily circular) quantum dots with Coulomb interaction (in dipole approximation) between the dots. We provide an overview over the state of art of these systems which includes the results of former publications. References can be found in the text.

- Similar to single dots, the center-of-mass coordinates of all dots can be separated from the relative coordinates. Only the c.m. coordinates of different dots are coupled to each other. The relative coordinates of different dots are neither coupled to each other nor to the c.m. coordinates.
- This gives rise to two types of excitations: two collective c.m. modes per dot and and a complex spectrum of intradot excitations. In periodic arrays only the collective c.m. modes show dispersion. Intradot excitations are dispersionless.
- The c.m. system can be solved exactly and analytically providing magnetophonon excitations characterized by a certain wave number $\mathbf{q}$ within the Brillouin zone. For $\mathbf{q}=0$ and one dot per unit cell, interdot interaction does not have any influence on the c.m. excitations.
- All dipole allowed excitations (seen in FIR experiments) are not influenced by the dot interaction.
- Interdot interaction between two dots influences the spectrum through a single parameter $p=2N\beta/a^3$, where a is the distance between the dots, N the number of electrons per dot and β the inverse background dielectric constant.
- If p exceeds a certain critical value p_{cr}, the lowest c.m. mode becomes soft leading to an instability. This transition is independent of the magnetic field.
- For $B=0$ and and one circular dot per unit cell, the two c.m. modes are not only degenerate in the middle of the Brillouin zone, but also at some points on the surface. If we use the NN approximation for the lattice sums in the dynamical matrix, degeneracy is maintained even on full curves in the Brillouin zone.
- Intradot excitations have to be calculated from an effective confinement. In circular dots with a cubic environment in nearest-neighbor approximation the effective confinement frequency reads $\omega_{0,eff}^2=\omega_0^2+2p$. This effective confinement differs from that for the c.m. motion.
- For p well below p_{cr}, the lowest intradot excitations are much smaller than the lowest collective excitations.
- The intradot excitation energies versus magnetic field exhibit kinks at those fields, where the angular momentum of the ground state changes.

In the Appendix we prove a Kohn theorem for dot arrays with Coulomb interaction between the dots without the dipole approximation. The individual confinement potentials can be arbitrarily arranged and can carry different electron numbers, but have to be described by identical confinement tensors. This means that for breaking Kohn's theorem in dot arrays, we have to have at least two different confinement species.

ACKNOWLEDGMENTS

I am indebted to D. Heitmann, H. Eschrig, and E. Zaremba and their groups for very helpful discussion and the

Deutsche Forschungs-Gemeinschaft for financial funding.

APPENDIX

We are going to prove that for an arbitrary array (the dot centers can be arranged arbitrarily) of identical parabolic quantum dot potentials (the confinement tensors $\mathbf{\Omega}$ of all dots must be equal) in an homogeneous magnetic field: (i) the total c.m. degree of freedom can be separated from the rest, (ii) the total c.m. Hamiltonian is not influenced by Coulomb interaction, and (iii) the eigenvalues of the total c.m. Hamiltonian are independent of the electron number N in each dot (the electron number in different dots can be different).

The Hamiltonian $H=H^{(0)}+V$ consists of an one-particle term $H=H^{(0)}$ and the Coulomb interaction between all electrons V. The dot centers are located at $\mathbf{R}_\alpha^{(0)}$ and the electron coordinates are denoted by $\mathbf{r}_{i\alpha}=\mathbf{R}_\alpha^{(0)}+\mathbf{u}_{i\alpha}$. Then we have

$$H^{(0)}=\sum_{i\alpha}\left\{\frac{1}{2m^*}\left[\mathbf{p}_{i\alpha}+\frac{1}{c}\mathbf{A}(\mathbf{R}_\alpha^{(0)}+\mathbf{u}_{i\alpha})\right]^2+\frac{1}{2}\mathbf{u}_{i\alpha}\cdot\mathbf{C}\cdot\mathbf{u}_{i\alpha}\right\}. \tag{A1}$$

First of all, we shift the gauge center for each electron into the middle of the corresponding dot using an unitary transformation similar to Eq. (16). This transforms the shift $\mathbf{R}_\alpha^{(0)}$ in the argument of the vector potential away. Next we drop the index α in Eq. (A1) so that the index ''i'' runs over all electrons in all dots. Now we perform a transformation to new coordinates $\tilde{\mathbf{u}}_i$:

$$\mathbf{u}_i=\sum_k Q_{ik}(\sqrt{N}\,\tilde{\mathbf{u}}_k);\quad (\sqrt{N}\,\tilde{\mathbf{u}}_i)=\sum_k Q_{ki}^*\mathbf{u}_k, \tag{A2}$$

where Q_{ik} is an unitary matrix. This implies

$$\mathbf{p}_i=\sum_k Q_{ik}^*\left(\frac{\tilde{\mathbf{p}}_k}{\sqrt{N}}\right);\quad \left(\frac{\tilde{\mathbf{p}}_i}{\sqrt{N}}\right)=\sum_k Q_{ki}\mathbf{p}_k. \tag{A3}$$

It is possible to choose for the first column $Q_{k1}=1/\sqrt{N}$. The other columns need not be specified. Then $\tilde{\mathbf{u}}_1=(1/N)\Sigma_i\mathbf{u}_i=\mathbf{U}$ is the c.m. of all elongations, or, the c.m. of the electron coordinates with respect to the weighted center of the dot locations $\mathbf{R}^{(0)}=(1/N)\Sigma_\alpha N_\alpha\mathbf{R}_\alpha^{(0)}$, where N_α is the number of electrons in dot α. The corresponding canonical momentum $\tilde{\mathbf{p}}_1=(1/i)\nabla_{\tilde{\mathbf{u}}_1}=\mathbf{P}$ is the c.m. momentum. Inserting our transformation into Eq. (A1) provides

$$H^{(0)}=\sum_i\left\{\frac{1}{2m^*}\left[\frac{1}{\sqrt{N}}\tilde{\mathbf{p}}_i+\sqrt{\frac{N}{c}}\mathbf{A}(\tilde{\mathbf{u}}_i)\right]^2+\frac{N}{2}\tilde{\mathbf{u}}_i\cdot\mathbf{C}\cdot\tilde{\mathbf{u}}_i\right\} \tag{A4}$$

The term $i=1$ in Eq. (A4) is the (separated) c.m. Hamiltonian

$$H_{c.m.}=\frac{1}{2m^*}\left[\frac{1}{\sqrt{N}}\tilde{\mathbf{P}}+\sqrt{\frac{N}{c}}\mathbf{A}(\tilde{\mathbf{U}})\right]^2+\frac{N}{2}\tilde{\mathbf{U}}\cdot\mathbf{C}\cdot\tilde{\mathbf{U}} \tag{A5}$$

which agrees with Eq. (10). Clearly, the Coulomb interaction V in H is independent of the c.m., and does not contribute to $H_{c.m.}$. For the independence of the eigenvalues of N see the discussion following Eq. (10).

This proof, in particular the step from Eqs. (A1) to (A4), is not correct if the dot confinement tensor $\mathbf{C}$ depends on α (or ''i'' in the changed notation). Therefore all dots must have the same $\mathbf{C}$, but can have different electron numbers N_α. In other words, the total c.m. excitations in dot arrays, which are seen in FIR spectra, are not affected by the *e e* interaction, if and only if all confinement tensors $\mathbf{C}$ are equal. On the other hand, *if we want to observe e e interaction in the FIR spectra and break Kohn's theorem, we have to use dot lattices with at least two different confinement tensors*. The simplest way to implement this is using a lattice with two noncircular dots per cell, which are equal in shape, but rotated relative to each other by 90° (see Ref. 12).

*Email address: m.taut@ifw-dresden.de

[1] L. Jacak, P. Hawrylak, and A. Wojs, *Quantum Dots* (Springer, Berlin, 1998).

[2] K. Kempa, D.A. Broido, and P. Bakshi, Phys. Rev. B **43**, 9343 (1991); A.O. Govorov and A.V. Chaplik, Zh. Éksp. Teor. Fiz. [Sov. Phys. JETP **72**, 1037 (1991)]; J. Phys. C **6**, 6507 (1994); A.V. Chaplik and A.O. Govorov, *ibid.* **8**, 4071 (1996).

[3] J. Dempsey, N.F. Johnson, L. Brey, and B.I. Halperin, Phys. Rev. B **42**, 11 708 (1990).

[4] T. Chakraborty, V. Halonen, and P. Pietiläinen, Phys. Rev. B **43**, 14 289 (1991).

[5] P.A. Maksym, Physica B **249**, 233 (1998); O. Dippel, P. Schmelcher, and L.S. Cederbaum, Phys. Rev. A **49**, 4415 (1994); B. Schuh, J. Phys. A **18**, 803 (1985).

[6] C. Tsallis, J. Math. Phys. **19**, 277 (1978); Y. Tikoshinsky, *ibid.* **20**, 406 (1979).

[7] M. Taut, J. Phys. A **27**, 1045 (1994); **27**, 4723(E) (1994). Additionally, in formula (10) in the term containing $\partial/\partial\alpha$ a factor $\frac{1}{2}$ is missing, and on the right-hand side of Eqs. (19a) and (20a) $\tilde{\omega}$ must be replaced by $\tilde{\omega}_r$.

[8] U. Merkt, J. Huser, and M. Wagner, Phys. Rev. B **43**, 7320 (1991); M. Wagner, U. Merkt, and A.V. Chaplik, *ibid.* **45**, 1951 (1992).

[9] P.A. Maksym and T. Chakraborty, Phys. Rev. Lett. **65**, 108 (1990); Phys. Rev. B **45**, 1947 (1992); P.A. Maksym, Physica B **184**, 385 (1993).

[10] C. Schüller, K. Keller, G. Biese, E. Ullrichs, L. Rolf, C. Steinebach, and D. Heitmann, Phys. Rev. Lett. **80**, 2673 (1998).

[11] C. Dahl, J.P. Kotthaus, H. Nickel, and W. Schlapp, Phys. Rev. B **46**, 15 590 (1992).

[12] M. Taut, cond-mat/0007054 (unpublished).